

Determining the Spectral Content of MOSES Images

Jacob D. Parker¹ · Charles C. Kankelborg¹

© Springer •••

Abstract

Keywords: Need to look through the list of allowed keywords and pick a couple

1. Introduction

1.1. Temporary Outline

1. Brief discussion of TR and events worth studying
2. Cite previous studies the TR and motivate MOSES
3. Briefly describe instrument concept but mostly cite previous works on this.
4. Possibly cite the scientific success of Skylab overlapograms to prove the utility of this type of data.
5. Point to EIS Slot Paper by MSSL folk
6. Outline the rest of the paper.

2. Data

The Multi-Order Solar EUV Spectrograph (MOSES) sounding rocket launched from White Sands Missile Range on February 8th, 2006 at 18:44 UT. It recorded 27 exposures between 18:44:17 and 18:49:13 UT above 160 km in altitude. Exposure times ranged from .25 - 24 seconds with a roughly 6 second readout time in between. An exposure consists of three images, one for each of the three spectral orders $m = -1, 0, \text{ and } 1$. All data was dark subtracted and co-aligned to exposure number 13 prior to our study (Fox, Kankelborg, and Thomas, 2010; Fox, 2011; Rust, 2017).

✉ J.D. Parker
jacob.parker3@montana.edu
C.C. Kankelborg
want to include your email charles?

¹ Montana State University

Of the different exposures, longer exposures are best for observing quiet sun features but are saturated near active regions. To fill in missing saturated regions and increase signal to noise we form a single time averaged image in all three spectral orders. Saturated pixels are masked with NaNs (Not a Number) and treated as missing data. Since MOSES observes through changing amounts of atmosphere throughout its flight we use the median of each image as a synthetic exposure time, rather than the amount of time the shutter is open. Masked data is then summed in time and divided by a total synthetic exposure time for each pixel to form a single time averaged image in each spectral order with no saturated pixels. Figures 1a and 1b shows the $m = 0$ and 1 order time averaged images.

Identifying solar features in the MOSES data that have undergone spectral dispersion is simple. Subtracting the $m = 0$ image (that contains no spectral dispersion) from either outboard order eliminates non-dispersed features. What remains are bi-polar features of various spatial scales. A feature in the principle wavelength, He II $\lambda 303.8\text{\AA}$, with a nonzero line-of-sight (LOS) velocity is translated along image rows. MOSES has a spectral dispersion of $\approx 30 \text{ km s}^{-1} \text{ pixel}^{-1}$, leading to a less than ten pixel shift for even the fastest LOS velocities in He II. This results in a bi-polar feature with an obvious positive and negative counterpart that are immediately next to one another. Events like these have been studied in detail by several authors (Fox, Kankelborg, and Thomas, 2010; Rust, 2017; Courrier and Kankelborg, 2018).

Features from other emission lines in the MOSES passband have shifts larger than 10 pixels and cannot be mistaken as Doppler shifted features in He II $\lambda 303.8\text{\AA}$. A feature in Si XI $\lambda 303.3\text{\AA}$, the next closest line, would be shifted by 17 pixels. Si XI features can be seen on the solar limb where He II has little to no contribution. The best example of this is seen in box 3 of Figure 1c. Box 1 of Figure 1c has a large, coherent, negative feature dubbed the “wishbone”. The wishbone is very solar in appearance and has no obvious positive counterpart. Close inspection reveals a white smear to its left that is likely a shifted wishbone in the plus order. Unfortunately the positive portion of the wishbone is too blurry to quantify its shift by inspection. A previous study of these features by Rust (2017) used a wavelet transform to isolate large scale features prior to taking the difference. That procedure allowed Rust (2017) to roughly identify a contribution from Mg VII $\lambda 315\text{\AA}$ to regions 1 and 2 and from Si IX/ Fe VI $\lambda 296.1\text{\AA}$ to region 3 of Figure 1c. .

In support of the 2008 MOSES rocket flight the EUV Imaging Telescope (EIT) (Delaboudinière *et al.*, 1995) on board SOHO (?) captured 4 full disk EUV images, one in each of the 171 \AA , 195 \AA , 284 \AA , and 304 \AA channels 2. Each image was first despiked via `iris_prep_despike.pro` with default settings and made level 1 via `eit_prep.pro`. They were then rotated to 2006-02-08 18:47 UT, the timestamp of image 13 of the MOSES observing sequence (Fox, 2011), and rebinned to the MOSES angular resolution of 0.59 arcsec per pixel. Each image was co-aligned to MOSES via the cross correlation of the MOSES $m = 0$ image and EIT 304 \AA channel. At first glance one can find several similar feature in the MOSES difference image (Figure 1c) and the EIT 171, 195, and 284 images

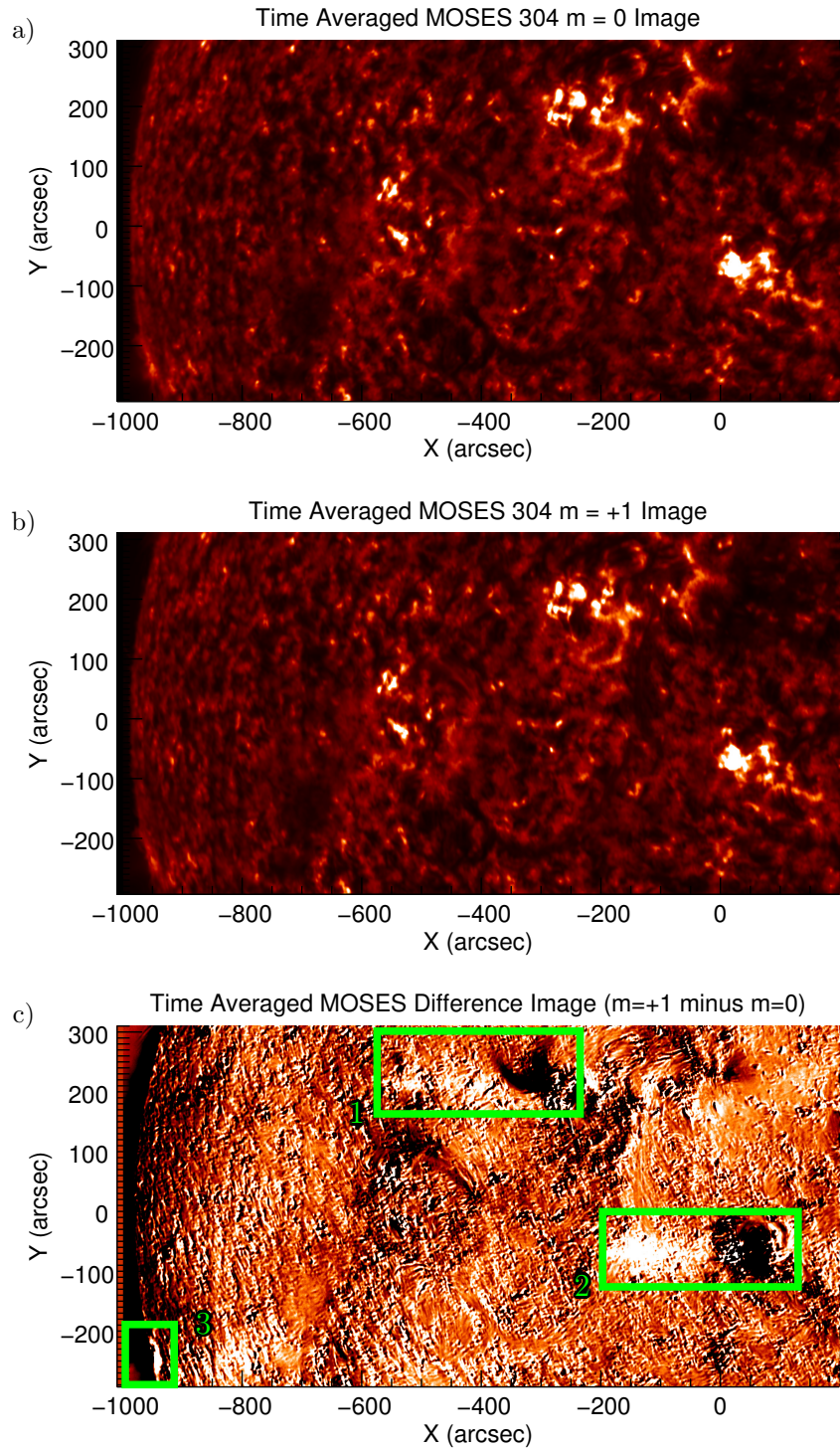


Figure 1. Time averaged images for the $m = 0$ (a) and 1 (b) spectral orders, followed by their difference (c), $m = 1$ minus $m = 0$. Regions one through three, boxed in green, show regions of high spectral contamination. Dark features from the $m = 0$ order are adjacent to white smears with pixel shifts too large to be Doppler shifts.

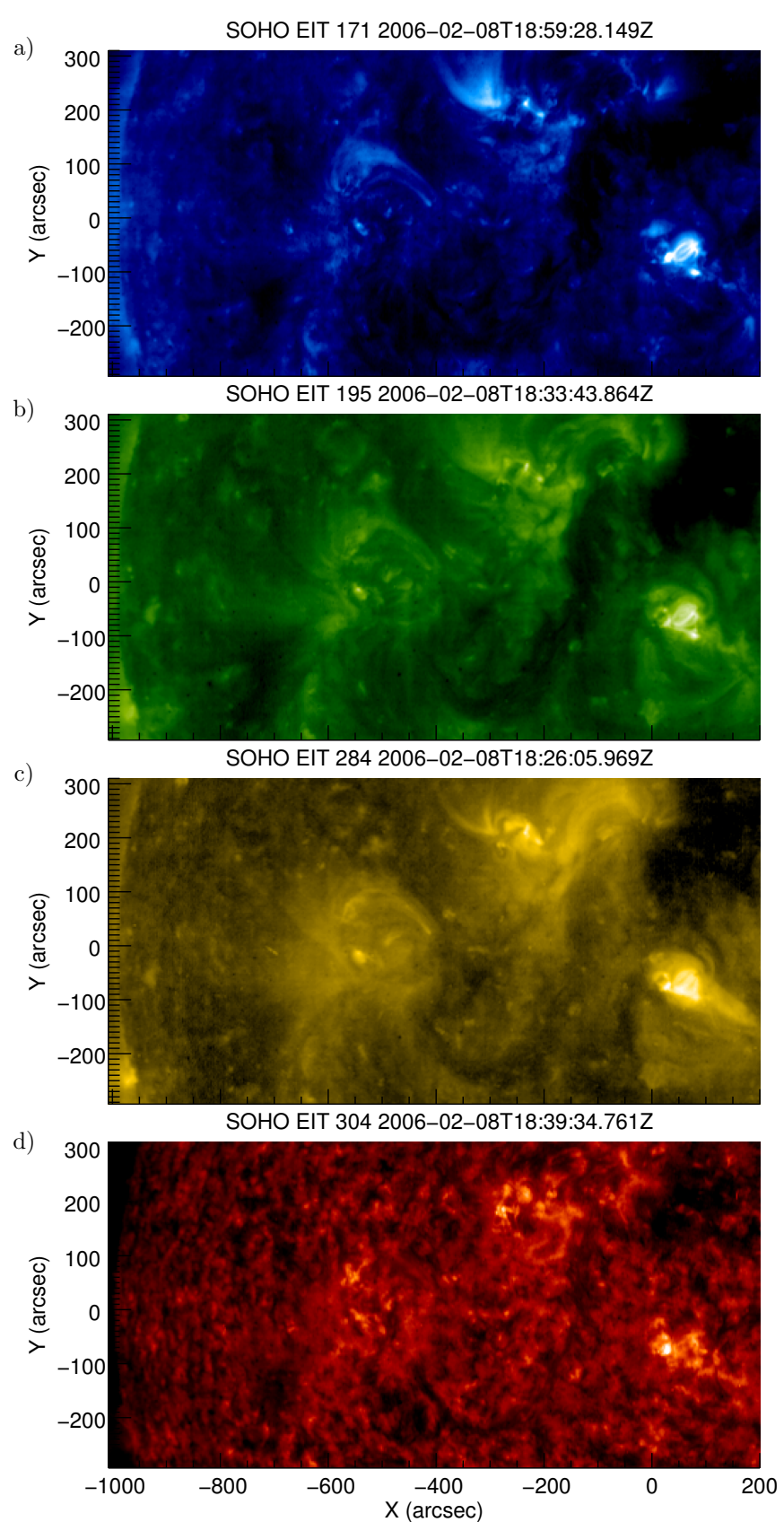


Figure 2. SOHO EIT Images taken closest the MOSES Launch. Each channel has been rebinned to match MOSES angular resolution and co-aligned to the MOSES FOV

(Figure 2a, 2b, 2c). The presence of these features in MOSES data indicates a contribution of coronal spectral lines to an otherwise transition region image.

While similarities between MOSES difference images and EIT images indicate the contribution of hotter lines to MOSES He II data, they do not tell how much, and by which lines. In Section 3 we use cross-correlation, and a forward model of the MOSES instrument that utilizes the EIT images from Figure 2 and Chianti (?) to identify the contamination lines within the MOSES passband, and the extent of their contribution to MOSES images.

JDP: Question, if I rotate an image to a specific time, do I maintain the original time stamp in Figure 2, do I not display it at all, or do I label it with the new time it has been rotated to?

3. Methods

3.1. Temporary Outline

I am having trouble organizing my thoughts for this section. Lets try this way.

1. Summary
2. Cross Correlation
 - a) Cross Correlation Equations
 - b) Why Difference Images
 - c) Show Cross-Correlation Function
3. Significance Testing
 - a) Looking for Significant Peaks in Correlation
 - b) Columns (No Spectral Dispersion)
 - c) Building Longer Columns in Fourier Space
 - d) Phase Shuffling for Random Data
 - e) Correlation Length for Degrees of Freedom
4. Forward Model
 - a) Synthetic MOSES images for different DEMs
 - b) Coaligned EIT Images
 - c) Chianti Temperature Image Selection and Intensity
 - d) MOSES PSF Convolution
 - e) Linear Combination and Least Squares Minimization with MCMC

3.2. Cross-Correlation

CCK: I think this paragraph could be at the head of the subsection. I think it would also be appropriate to mention that we have *tried* cross-correlating the orders. Perhaps it is worth showing the results and explaining what we can see in them, but why they are uninformative for the question of off-band emission. The He II component dominates that cross-correlation so completely, and across such a wide range of scales, that the contributions of the minor players is obscured.

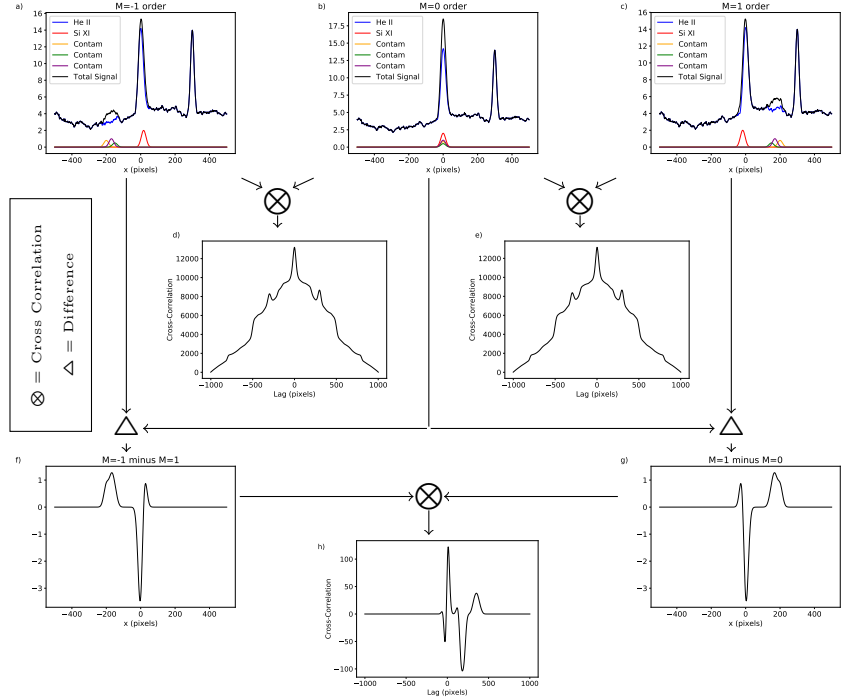


Figure 3. A graphical representation of our cross-correlation procedure

JDP: My intention is to demonstrate the side effects of cross-correlating individual orders in Figure 3. This cartoon is still incomplete, but I believe if I add a simple He II background that the dominance of He II autocorrelation will be easy to see. Let me know how you feel about the new arrangement of paragraphs.
CCK: yes, I think this order is logical.

To help identify subtle pattern repetition in the MOSES difference images we cross-correlated them along the dispersion direction, or image rows. Preforming a cross-correlation on the difference images requires justification. An obvious first choice would have been to simply cross-correlate the $m = 0$ order with either outboard order. Unfortunately the correlation function is dominated by the autocorrelation of the He II signal as seen in Figure 3 (**LETTER**). This would also be the case when cross-correlating the $m = 1$ and $m = -1$ order images. By taking the difference we remove stationary He II objects from the images and in turn their autocorrelation from the cross-correlation functions.

JDP: I believe I can better illustrate these points with a tuned version of Figure 3
CCK: Yes, makes sense.

The cross-correlation of two difference images is defined to be,

$$PZ \otimes MZ = \mathcal{F}^{-1} \{ \mathcal{F}(PZ) * \mathcal{F}(MZ) \}, \quad (1)$$

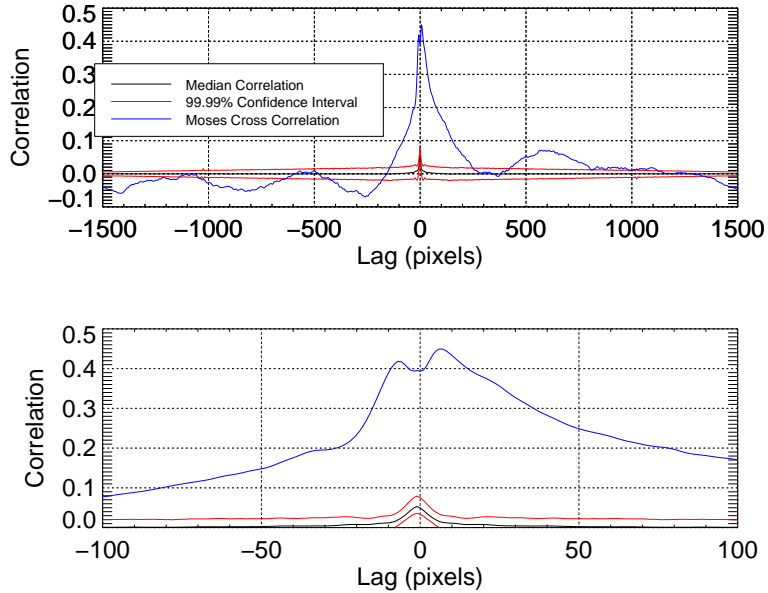


Figure 4. The mean cross-correlation function of MOSES difference image rows (blue) overlaid on the 99.99 percent confidence interval formed by cross-correlating random data (red).

CCK: Might be simpler to just use $P - Z$ and $M - Z$; less to explain. where PZ and MZ are the $m = 0$ order subtracted from the $m = 1$ order and the $m = 0$ order subtracted from the $m = -1$ order respectively. \mathcal{F} is the Fast Fourier Transform (FFT) operator. The MOSES image rows were also Hanning windowed, and padded with zeros, prior to applying the FFT to minimize edge effects. The discrete Hanning window, $w(l)$, implemented was,

$$w(l) = \alpha - (1 - \alpha)\cos\left(\frac{2\pi l}{N}\right) \text{ for } l = 0, 1, \dots, N - 1 , \quad (2)$$

where N is the number of elements in the array being windowed and $\alpha = .5$.

This procedure yields a one dimensional cross-correlation function for each row of the MOSES difference images. Since we are concerned mostly with bulk spectral content we then take the mean of all 1024 cross-correlation functions, one for each row, to get our final correlation curve plotted in blue in Figure 4.

The cross-correlation curve or the MOSES difference images has a few notable features. There are noticeable peaks in correlation at approximately -800 , 250 , and $+600$ pixel lags. The largest peak in correlation, centered about zero lag, also displays a double peak, not typical of cross-correlation functions that generally have maxima at zero lag for uncorrelated functions. CCK: Autocorrelations

have unity peaks at zero lag; but what should be our expectations of a cross-correlation? JDP: Error on my part. Cross correlations (and auto-correlations) of uncorrelated functions tend to have maxima at zero lag when using a fixed mean subtraction. CCK: Hm. That still does not sound correct. While these features are identifiable, the curve is complicated enough that quantifying peaks in correlation visually is difficult and the significance of any given peak is questionable. We therefore move to test the null hypothesis that none of these features are statistically significant by cross-correlating random data generated to match the MOSES image rows.

3.3. Significance Testing

CCK: Try to explain this hypothesis a bit more clearly. Describe step by step how spectral lines different from the dominant He II line could give rise to such peaks. JDP: I agree that I need to illustrate this somewhere, maybe its better to explain this is Section 3.2? I am struggling to fit it here because it has nothing to do with significance testing. CCK: Agreed. Top of 3.2 perhaps?

CCK: Slow down a bit. We cannot test the hypothesis directly. We instead seek to exclude a null hypothesis, that the peaks in our difference image cross-correlations are due to a happenstance combination of solar features in He II rather than features shifted by dispersion. We believe this to be the most likely alternative to our proposed hypothesis. To test the null hypothesis, we need a dataset that represents the null hypothesis. The null hypothesis dataset needs to be large enough, and have enough random variations, to gather statistics that represent what is possible under the null hypothesis...

JDP: Correct, my language was imprecise. I will make this more clear.

The mean cross-correlation function of the two MOSES difference images, blue in Figure 4, has several peaks at nonzero lags.

To reject the null hypothesis we cross correlated randomly generated synthetic solar data that matched MOSES image rows in length and had similar power spectral and autocorrelation distributions. Our test data set was generated from the MOSES image columns because they contain the same solar features as the image rows, but contain practically no spectral dispersion. By interpolating and shuffling the elements of the MOSES columns in Fourier space we can generate a large number of test arrays for significance testing.

MOSES images contain 2048 columns. These columns have the same spatial features as MOSES image rows but with none of the spectral information. Despite this the MOSES image columns are insufficient for significance testing in a couple ways. First, there is an insufficient sample size. With features in the MOSES images ranging from four to about a hundred pixels we have at most 512 unique columns for significance testing. Second, they are half as long as the rows, preventing us from measuring the significance of correlation past 1024 pixel lag. Therefore we needed to generate a synthetic data set for significance testing.

Using the MOSES image columns as our basis we generated N random arrays that are 2048 long and match MOSES columns in both power spectral and auto-correlation distribution. First the columns in each image, $P(x, y)$, $Z(x, y)$, and

$M(x, y)$, are windowed with a Hanning window, $w(y)$ (Equation 2), and Fourier transformed along the column dimension, y . The windowed Fourier transformed array is defined to be

$$\tilde{Z}_w[x, k] = \mathcal{F}_y [w(y)Z[x, y]], \quad (3)$$

where, $x = 0, 1, \dots, 2047$ and $y = 0, 1, \dots, 1023$. In Equation 3 and the following equations we will show the procedure used to generate random arrays for only the zero order, $Z(x, y)$, for simplicity even though an identical procedure was carried out on every order.

The transformation outlined in Equation 3 gives us 511 spatial frequency bins and one DC bin that each have 1024 elements, one for each column, for each order. Each new array, \tilde{Z}' , is formed by picking an element randomly from each frequency bin CCK: I know what you mean, but I don't think it is clear. Slow down. From the set of all the Fourier transformed data columns, we will generate a synthetic row, $Z'(x)$ by populating its Fourier transform, \tilde{Z}' . To further scramble the array each value of k , aside from the DC term, is given a random phase shift, $e^{i\phi}$. By this method the k^{th} element in each new synthetic array, \tilde{Z}'_k , is found as follows:

$$\tilde{Z}'_k = \tilde{Z}_w [\sigma(m, 2048), k] e^{i\Phi(n)}, \quad (4)$$

where,

$$\sigma(m, L) = \text{floor}\{\text{randomu}(m) * L\}, \quad (5)$$

$$\Phi(n) = 2\pi * \text{randomu}(n), \quad (6)$$

the function `randomu()` picks a random value from a uniform distribution between zero and one each time it is called, and `floor()` rounds down to the nearest integer. The function $\sigma()$ generates a random integer between zero and $L - 1$.

In order to create an array that is 2048 elements long from one that is 1024 elements long we require twice as many values of k . We solve this problem by double picking values from the distribution for each wave number, k . The values of k used in Equation 4 are,

$$k_j = \text{floor}(j/2), \quad (7)$$

where $j = 1, 2, \dots, 1022$. Since our data is purely real we can fill in the remaining Fourier components, negative frequencies, with the complex conjugate of the corresponding positive frequency component. The final synthetic MOSES row is found through a FFT,

$$Z' = \mathcal{F}_y^{-1}[\tilde{Z}']. \quad (8)$$

To verify that our N synthetic arrays match the MOSES columns we take a 1024 element long section of each synthetic array, as well as the MOSES columns,

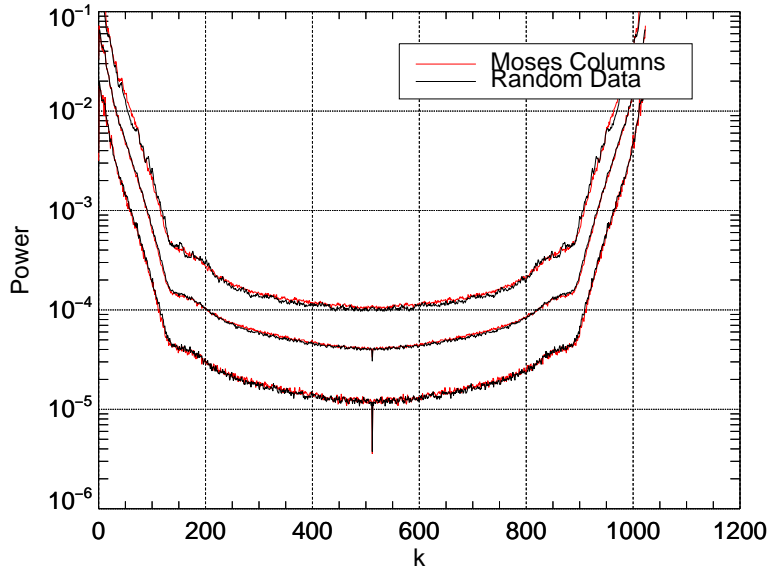


Figure 5. The 10th, 50th, and 90th percentile of the power spectral distribution for each value of k is plotted for both the MOSES columns and synthetic data.

and plot portions the power spectral and autocorrelation distributions. Figures 5 and 6 show three percentiles of the distribution (10th, 50th, and 90th) for both power spectra and autocorrelation for N equal to 10,000 synthetic arrays. Figure 5 shows great agreement between synthetic data and the MOSES columns in power spectral distribution. Figure 6 show good agreement between the synthetic data and MOSES columns at the median and only marginal agreement in the wings of the distribution. Despite that the synthetic data always has a high autocorrelation length that the MOSES columns and therefore acts as a worse case scenario during significance testing.

Figure 4 shows the results of our significance testing with 10,000 synthetic arrays. Each set of three arrays, Z' , M' and P' , are subtracted and correlated according to Equation 1. CCK: I think you left something out. Don't you actually generate Z' , M' and P' in parallel, choosing the same x -index for each k in all 3 arrays? Otherwise you'd have a different synthetic sun in each array, so the analogy to the MOSES data would not be so good. JDP: Correct, I attempted to state this at the start of the methods section but will make this more clear. We find that the mean cross-correlation of MOSES difference images along their rows has peaks that are much greater than the 99.99% confidence interval and are therefore significant and indicative of extra spectral content. CCK: It may be worth discussing the properties of the synthetic rows in more detail. Not all of the following are necessarily important; somewhat in brainstorming mode

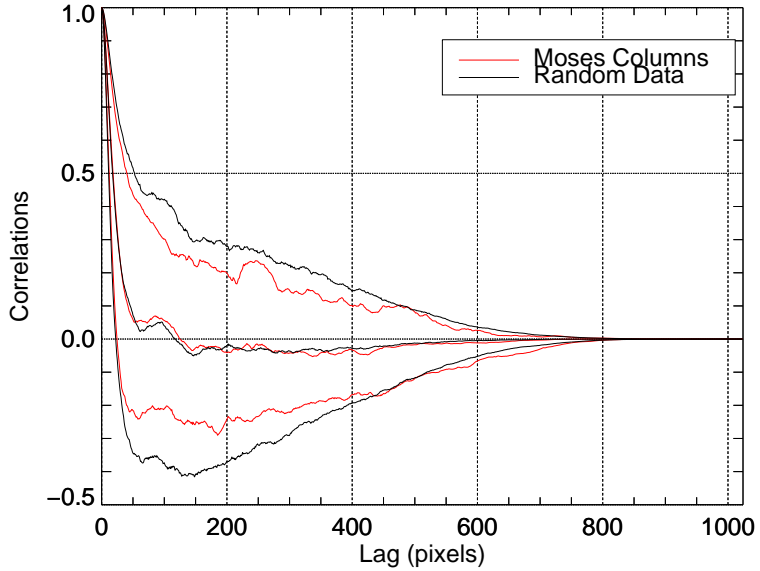


Figure 6. The 10th, 50th, and 90th percentile of the autocorrelation distribution for each value of k is plotted for both the MOSES columns and synthetic data.

here. Are the synthetic data positive definite? Does it matter (probably not)? Do the rows show similar power spectra? How might the synthetic data may differ from the real thing, in ways other than the spectral lines we are looking for? For example, there are also line profile and PSF effects. This could change the structure near zero lag, but the effective range of these features is probably small (how many pixels?).

CCK: Are we comparing difference cc lags for one synthetic column to an average of difference cc lags for 1024 rows? What is the implication of that?
 JDP: The idea of Figures 7 and 8 is to show that a 1024 section of the randomly generated data matches certain characteristics of an actual MOSES column. These plots show that the synthetic date matches the distribution of MOSES columns, not just the average. CCK: Nice. Just need some discussion to go with.

3.4. Forward Model

The mean cross-correlation of MOSES difference image rows is shown in Figure 4. In Section 3.3 several peaks in correlation were deemed to be significant and indicative of extra spectral content in the MOSES data. These peaks have irregular, broad profiles and are both positive and negative. To interpret how these peaks in correlation relate to spectral content we developed a forward model that produces synthetic MOSES difference images with known spectral content using Chianti () and images from EIT ().

3.5. Fitting

Using a MCMC to thoroughly explore the parameter space and generate error bars on fit parameters. More work to be done here.

4. Results

Synthetic images of best fit. Quantify extra spectral content. Comment on extra He II emission unaccounted for by Chianti.

5. Discussions/Conclusions

Implications for future, design changes incorporated in ESIS (field stop, line selection, dispersion increase?). Possibly examine the spectra surrounding Ne VII 465 Å. Do we have the MOSES II throughput curves?

References

- Courrier, H.T., Kankelborg, C.C.: 2018, Using local correlation tracking to recover solar spectral information from a slitless spectrograph. *Journal of Astronomical Telescopes, Instruments, and Systems* **4**, 018001. DOI. [[Courrier2018](#)]
- Delaboudinière, J.-P., Artzner, G.E., Brunaud, J., Gabriel, A.H., Hochedez, J.F., Millier, F., Song, X.Y., Au, B., Dere, K.P., Howard, R.A., Kreplin, R., Michels, D.J., Moses, J.D., Defise, J.M., Jamar, C., Rochus, P., Chauvineau, J.P., Marioge, J.P., Catura, R.C., Lemen, J.R., Shing, L., Stern, R.A., Gurman, J.B., Neupert, W.M., Maucherat, A., Clette, F., Cugnon, P., van Dessel, E.L.: 1995, EIT: Extreme-Ultraviolet Imaging Telescope for the SOHO Mission. *Sol. Phys.* **162**, 291. DOI. [[EIT](#)]
- Fox, J.L.: 2011, Snapshot imaging spectroscopy of the solar transition region: The Multi- Order Solar EUV Spectrograph (MOSES) sounding rocket mission. PhD thesis, Montana State University. ADS. [[Fox2011](#)]
- Fox, J.L., Kankelborg, C.C., Thomas, R.J.: 2010, A Transition Region Explosive Event Observed in He II with the MOSES Sounding Rocket. ??*jnlApJ* **719**, 1132. DOI. ADS. [[Fox2010](#)]
- Rust, T.L.: 2017, Explosive Events in the Quiet Sun: Extreme Ultraviolet Imaging Spectroscopy Instrumentation and Observations. PhD thesis, Montana State University. ADS. [[Rust2017](#)]

6. Acronyms

MOSES Multi-Order Solar EUV Spectrograph

EIT EUV Imaging Telescope